Microvascular Research 141 (2022) 104317

Contents lists available at ScienceDirect

Microvascular Research

journal homepage: www.elsevier.com/locate/ymvre

Comprehensive imaging of microcirculatory changes in the foot during endovascular intervention – A technical feasibility study

Martin Hultman [a,*], Sofie Aronsson [b], Ingemar Fredriksson [a,c], Helene Zachrisson [b,d], Håkan Pärsson [e], Marcus Larsson [a], Tomas Strömberg [a]

[a] Department of Biomedical Engineering, Linköping University, Linköping, Sweden
[b] Department of Health, Medicine, and Caring Sciences, Division of Diagnostics and Specialist Medicine, Linköping University, Linköping, Sweden
[c] Perimed AB, Datavägen 9A, Järfälla, Stockholm, Sweden
[d] Department of Clinical Physiology, Linköping University Hospital, Linköping, Sweden
[e] Department of Biomedical and Clinical Sciences, Linköping University, Linköping, Sweden

ARTICLE INFO

Keywords:
Chronic limb-threatening ischemia
Microcirculation
Multi-exposure laser speckle contrast imaging
Multi-spectral imaging

ABSTRACT

Chronic limb-threatening ischemia (CLTI) has a major impact on patients' lives and is associated with a heavy health care burden with high morbidity and mortality. Treatment by endovascular intervention is mostly based on macrocirculatory information from angiography and does not consider the microcirculation. Despite successful endovascular intervention according to angiographic criteria, a proportion of patients fail to heal ischemic lesions. This might be due to impaired microvascular perfusion and variations in the supply to different angiosomes. Non-invasive optical techniques for microcirculatory perfusion and oxygen saturation imaging have the potential to provide the interventionist with additional information in real-time, supporting clinical decisions during the intervention. This study presents a novel multimodal imaging system, based on multi-exposure laser speckle contrast imaging and multi-spectral imaging, for continuous use during endovascular intervention. The results during intervention display spatiotemporal changes in the microcirculation compatible with expected physiological reactions during balloon dilation, with initially induced ischemia followed by a restored perfusion, and local administration of a vasodilator inducing hyperemia. We also present perioperative and postoperative follow-up measurements with a pulsatile microcirculation perfusion. Finally, cases of spatial heterogeneity in the oxygen saturation and perfusion are discussed. In conclusion, this technical feasibility study shows the potential of the methodology to characterize changes in microcirculation before, during, and after endovascular intervention.

1. Introduction

Peripheral arterial disease (PAD) is a heavy health care burden and is difficult to treat. More than 200 million people around the world are affected (Shu and Santulli, 2018). Chronic limb threatening ischemia (CLTI) is the end-stage of PAD, involving rest pain and lower limb ulceration with more than two weeks duration or gangrene. CLTI is associated with impaired quality of life, risk of limb loss, and increased mortality. There is also a risk for reinterventions (Conte et al., 2019), reported as high as 60% within 6 months (Duff et al., 2019), indicating that despite improved macrocirculation, the improvement in microcirculation is inadequate to allow for healing (Varela et al., 2017). This clearly shows the need for improved methods for PAD assessment and treatment follow-up.

Revascularization procedures in PAD use open by-pass surgery or endovascular intervention with percutaneous transluminal angioplasty (PTA) and stents to improve arterial blood flow. Before intervention, the larger vessels are generally evaluated by duplex ultrasound, CT-angiography, or MR-angiography, as well as ankle and toe blood pressures. In some centers, additional measurement of transcutaneous partial pressure of oxygen ($tcpO_2$) is performed (Conte et al., 2019; Gunnarsson et al., 2021).

Current feedback during CLTI surgery is based on angiography of larger vessel patency which only evaluates macrocirculation. This is a limited predictor of the underlying pathogenesis in non-healing ulcers. Therefore, for a complete vascular tree assessment, microcirculation

* Corresponding author.
E-mail address: martin.o.hultman@liu.se (M. Hultman).

https://doi.org/10.1016/j.mvr.2022.104317
Received 21 September 2021; Received in revised form 17 December 2021; Accepted 3 January 2022
Available online 10 January 2022

measurements have been proposed (Antonopoulos et al., 2019). Despite this, the current clinical use of microcirculatory evaluation is low or non-existent in daily clinical practice, possibly due to lack of integrated imaging methods. There are pointwise methods for assessing the microcirculation, such as $tcpO_2$ and skin perfusion pressure, but the spatial heterogeneity of the vascular anatomy in CLTI demands assessment of the microcirculation in the whole foot (Misra et al., 2019). Improved imaging modalities are therefore warranted.

Laser speckle contrast imaging (LSCI) (Boas and Dunn, 2010) and multi-spectral imaging (MSI) (Guolan and Baowei, 2014) are non-invasive methods for measuring spatial maps of microcirculatory perfusion and oxygen saturation, respectively. Both methods have previously been used to assess the microcirculatory status in patients with PAD and/or CLTI. For example, LSCI has been used to detect PAD based on the perfusion response to provocations. Mennes et al. (2019) used an arterial occlusion-release provocation, as well as a leg-elevation provocation, to distinguish between patients with and without CLTI. Katsui et al. (2017) used a thermal load test to diagnose patients with and without CLTI, as well as to investigate improvements after revascularization (Katsui et al., 2018). LSCI has also been used to monitor the healing of diabetic foot ulcers (Jayanthy, 2014; Mennes et al., 2021). Studies comparing LSCI before and after endovascular intervention are few. Kikuchi et al. (2019) investigated the change in pulsatile strength of the LSCI perfusion after successful intervention and found that it was significantly improved. Similarly, MSI has been used to detect the presence and severity of PAD (Chiang et al., 2017) and has been shown to correlate positively with ankle-brachial index (ABI) (Chin et al., 2011). Several authors have also found that MSI can predict long-term healing of diabetic foot ulcers (Khaodhiar et al., 2007; Nouvong et al., 2009).

Notably missing from previous work is the use of LSCI or MSI during intervention to inform interventionist about peripheral tissue perfusion or oxygen saturation in real-time. Furthermore, previous studies have focused on either LSCI for perfusion or MSI for oxygen saturation, but simultaneous access to both quantities enable more comprehensive microcirculation imaging which can provide additional clinical value. In addition to this, a major disadvantage with LSCI is the ambiguous non-linear relation to perfusion by the more established technique laser Doppler flowmetry (LDF), as well as susceptibility to noise, which makes between-patient comparisons difficult (Hultman et al., 2020; Fredriksson et al., 2019; Humeau-Heurtier et al., 2013). We have recently developed a multi-exposure LSCI (MELSCI) technique with algorithms that can replace LDF by a video-rate modality (Hultman et al., 2020; Fredriksson et al., 2019), alleviating some of the issues with LSCI.

The aim of this study is to show the technical feasibility of assessing both microcirculatory perfusion and oxygen saturation during CLTI endovascular intervention using a novel integrated imaging technique. This will be demonstrated by presenting how spatiotemporal microcirculatory changes can be imaged at high resolution and speed during the intervention, especially targeting the response to provocations such as balloon occlusion and release as well as nitroglycerin induced vasodilatation. Successfully demonstrating this will enable further clinical studies.

2. Method

2.1. Study design

This prospective observational feasibility study was carried out at Linköping University Hospital, Department of Thoracic and Vascular Surgery. The inclusion criteria were a CLTI diagnosis, classified according to the Rutherford and WIfI scales (Hardman et al., 2014), as well as ABI. In total, four perioperative measurements were included, and a fifth was excluded. The interventions were guided by digital subtraction angiography. For two patients, measurements were also performed at a routine checkup 13 and 26 weeks after the intervention, respectively.

It should be noted that the patients were not under general anesthesia during the interventions. Thus, movements of the feet inevitably introduced movement artifacts in some measurements, although only parts of the measurements (not included in the results) were significantly disturbed by this. Furthermore, although the measurement setup in the operating theater allowed for real-time feedback, the interventionists did not partake of this information in the current study.

The study design was approved by the Regional Ethical Review Board in Linköping, Sweden (D.no. 2018/282-31), and written informed consent was obtained from the subjects before the measurements.

2.2. Multimodal imaging system and measurement setup

Measurements were done with two imaging modalities: MELSCI for perfusion images, and MSI for oxygen saturation images (Fig. 1). The imaging modalities MELSCI and MSI were integrated in a single system together with their respective light sources, a 785 nm laser for MELSCI and a white LED (SXA30-WHI, Smart vision light, MI, US) for MSI. The MELSCI camera was equipped with a 785 nm band-pass filter (55 nm FWHM, BN785, Midwest Optical Systems Inc., USA) to remove light in the visible spectrum from the LED. The imaging system was placed on the surgical table at 30–40 cm from the foot. This ensured that there were no motion artifacts due to the movement of the table during the procedure, and that the view of the foot was the same throughout. To allow an unobscured view of the foot, a hard-plastic cover was placed on the surgical table between the imaging system and the foot. The sterile cover was placed over the entire imaging setup. The plastic cover also had the effect of blocking out stray light from the surrounding equipment and room lighting, resulting in better image quality.

2.3. Multi-exposure laser speckle contrast imaging

Multi-exposure laser speckle contrast imaging (MELSCI) utilizes the laser speckle pattern caused by the light interaction with moving red blood cells to calculate spatial perfusion maps of the illuminated area (Briers et al., 2013). Specifically, the movement of the speckle pattern causes motion blur in the captured images, and the amount of blur is related to the average speed and amount of red blood cells. The amount of blur also changes with the exposure time of the images, where longer exposure-times result in more motion blur. MELSCI analyzes the local contrast (i.e. the opposite of blur) in images with different exposure time to compute a perfusion map over the image. Several models have been proposed for this (Parthasarathy et al., 2008; Thompson and Andrews, 2010; Zölei-Szénási et al., 2015), but common for these is that they require inverse fitting to map measured contrast to perfusion. This is time consuming when applied to images, and therefore not suitable for real-time feedback. We have recently demonstrated a MELSCI system that overcomes this drawback and enables real-time continuous measurements of perfusion images at framerates suitable for analyzing dynamic changes in the microcirculation (Hultman et al., 2020; Fredriksson et al., 2019; Hultman et al., 2017). Specifically, in this study we computed perfusion images of 320 × 256 pixels at 10 frames/s, continuously during the entire intervention. This enables both spatial and temporal analysis of the perfusion signal at all time-points.

2.4. Multi-spectral imaging

Multi-spectral imaging (MSI) can be used with white light illumination to extract information about the oxygenation state of hemoglobin based on the different absorption spectra of oxygenized and reduced hemoglobin paired with a sufficient spectral resolution. This allows for determining spatial maps of the blood oxygen saturation in tissue. In this study, a snapshot MSI camera (xiSpec MQ022HG-IM-SM4X4-VIS, XIMEA®, Germany) with 16 spectral bands between 450 and 650 nm was used. The design of the camera allowed for a simultaneous acquisition of all 16 spectral bands at high framerates. To reduce noise,

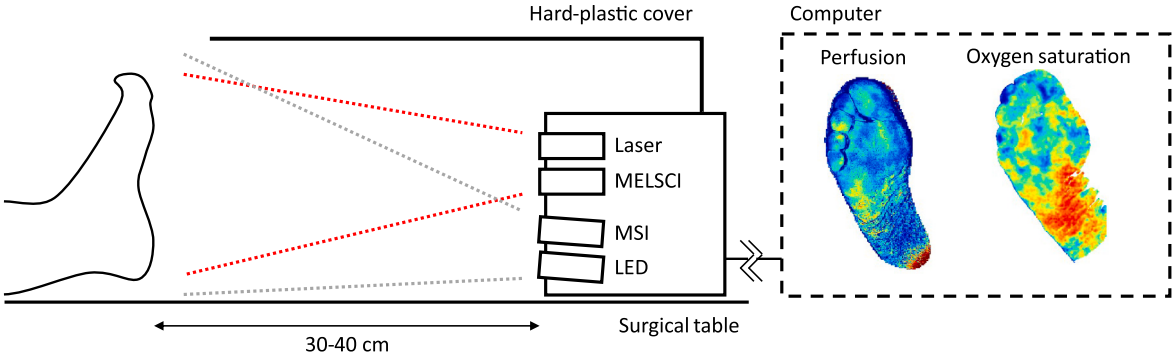

Fig. 1. Schematic overview of the multimodal imaging system and typical measurement setup during CLTI intervention surgery. Data were simultaneously recorded from two biooptical modalities; perfusion images from a MELSCI camera using a laser light source, and oxygen saturation images from an MSI camera with a LED light source. The cameras were placed directly on the surgical table at a distance of 30–40 cm from the foot. A hard-plastic cover was used to allow free line of sight to the foot at all times, and to block out stray light.

multiple consecutive images (i.e. multi-spectral data cubes) were averaged before being saved to disk, resulting in one averaged MSI data cube every fifth second. Ambient light images were acquired interleaved with these images, allowing for an effective subtraction of ambient light effects in the post processing.

Acquired images were analyzed using an algorithm based on artificial neural network (ANN) that was trained on a simulated data set that covers a large range of different tissue types. The use of realistic photon transport simulations in tissue using the Monte Carlo technique have previously been shown to enable an accurate estimation of tissue blood oxygen saturation from MSI data (Ewerlöf et al., 2021). By introducing ANN for solving the inverse problem, complete images of tissue blood oxygen saturation can be calculated and presented without any substantial computational delay (<0.1 s). Similar ANN approaches have previously proven both effective and accurate when estimating tissue blood oxygen saturation from diffuse reflectance spectra acquired using a probe-based system (Fredriksson et al., 2020).

2.5. Post-processing

The data was processed in three steps: background removal, region of interest (ROI) tracking and extraction, and motion artifact removal. The background in MELSCI images was removed using a deep learning UNet model for semantic segmentation (Öberg and Hulterström, 2021). For MSI images, the background was removed based on: 1) its spectral difference to normal tissue color; and 2) the variance in the saturation estimation from multiple trained ANN networks. The latter is a metric derived from the fact that background spectra are outside the ANN training space, thus causing relatively large variations in the output of multiple models.

ROIs were manually defined in three locations in the first frame of the recording. These locations were approximately the same in all subjects. For each subsequent frame, the position of the ROIs was calculated using an image registration algorithm implemented in Matlab 2021a (Mathworks, USA) to follow the motion of the foot (Öberg and Hulterström, 2021).

Large spikes in the graphs due to motion artifacts were removed using a local median filter. This affected only a small portion of the data but increased the readability of the results. The MELSCI perfusion images in the results were averaged over 2 s (20 frames), and perfusion graphs extracted from the ROIs were smoothed using a 5-second moving average filter (50 data points), unless explicitly stated otherwise. The larger averaging window in the graphs removed pulsatile information and noise, better revealed long term trends, and overall increased the clarity of the results. No additional smoothing was performed on the oxygen saturation images or ROIs.

3. Results

Four perioperative measurements are presented in this study, hereafter denoted Case 1–4. A fifth measurement was excluded due to excessive motion artifacts. The general labeling in the ROI graphs is according to *time* or *event*. Time-points selected for the perfusion and oxygen saturation images are labeled T_1, T_2, etc., and events in the intervention such as balloon dilations and deflations are labeled E_1, E_2, etc. ROIs are color-coded and labeled A, B, C. The locations of the ROIs are marked in each image, corresponding to the labeling shown in the first perfusion image.

Time-points were selected to highlight the spatiotemporal dynamics in the foot microcirculation in three categories. First, events in the intervention with known expected physiological reactions (Cases 1 and 2). Second, events with distinct changes in the microcirculation but with unknown causes (Cases 2, 3, and 4). Finally, measurements comparing the pulsatility between pre- and post-intervention measurements, as well as during a routine revisit (Cases 2 and 4).

A summary of clinical assessments performed at the pre- and post-intervention examinations, and revisit examination, is given in Table 1.

3.1. Case 1

The patient was a 64-year-old woman with a clinical history of ischemic heart disease, kidney failure, and diabetes. She had rest pain and ulcers (Rutherford 5). Fig. 2 shows the digital subtraction angiography images from (a) before, and (b) after the intervention. Selective angiography (Fig. 2a) showed stenosis in three vessels. The stenosis in

Table 1
Summary of patients and the clinical assessments performed before and after interventions, and at the revisit when applicable. ABI = ankle-brachial blood pressure ratio. Rutherford and WIfI scales are given in Hardman et al. (2014). W = wound, I=ischemia, inf = foot infection.

Patient	Sex	Age	Measurement	ABI [–]	Rutherford	WIfI [W,I, inf]
Case 1	F	64	Pre-op	0.76	5	2,3,1
			Post-op	1.1	–	–
Case 2	F	72	Pre-op	0	4	0,3,0
			Post-op	1.1	–	–
			Revisit (13 weeks)	0.87	1	0,0,0
Case 3	M	77	Pre-op	0	4	0,3,0
			Post-op	0.83	–	–
Case 4	M	71	Pre-op	0.29	4	0,3,0
			Post-op	0.80	–	–
			Revisit (26 weeks)	0.58	1	0,2,0

Fig. 2. Case 1. Digital subtraction angiography showing (a) stenosis in the superficial femoral artery, distal popliteal artery, and anterior tibial artery (red arrows). Restored arterial perfusion in the foot at the end of the intervention is shown in (b).

superficial femoral artery (SFA) was treated with 5 mm plain old balloon angioplasty (POBA), and the stenosis in the popliteal artery (segment p3) and the beginning of the anterior tibial artery were treated with 4 mm POBA and 2.5 mm drug-eluting balloon (DEB), respectively. Fig. 2b shows a restored arterial perfusion in the foot vessels. Angiography of the foot before the intervention was blurry due to motion artifacts and is therefore not included.

Fig. 3 shows the decrease and subsequent increase of perfusion and oxygen saturation during the application of a DEB dilation in the anterior tibial artery. The catheter was inserted in the anterior tibial artery at time E_1, causing a partial occlusion. The balloon was deflated at time E_2, indicated by an initial spike in perfusion and oxygen saturation, followed by a rapid reperfusion. Most notable is a net increase of oxygen saturation by approximately 30 percentage units in the 1st toe after the DEB dilatation, compared to the level before the insertion of the catheter (T_1). In addition, a smaller increase in oxygen saturation and perfusion can be seen in all ROIs and images. Note that this increase persisted for the remaining measurement period until the intervention was concluded at T = 1 h 50 min.

3.2. Case 2

The patient was a 72-year-old woman with a clinical history of smoking. She presented with ischemic rest pain, a 4 on the Rutherford scale. Preoperative duplex ultrasound showed an occlusion of the popliteal artery. Fig. 4 shows digital subtraction angiography from before (a-d) and after (e, f) the intervention. In (a) an occlusion in the superficial femoral artery can be seen, and in (b) an occlusion in the popliteal artery. An occlusion in the anterior tibial artery (c) is distally filling from collaterals as seen in (d). The occlusion in SFA was treated with woven self-expanding stents (5.5 × 200 mm and 4.5 × 80 mm) reaching to the popliteal artery (segment p3). A stenosis in the popliteal artery (segment p3), just distal to the stent, was treated with 4 mm DEB. The anterior tibial artery was occluded at the middle portion and was recanalized using 2.5 mm POBA. Successful recanalization of the anterior tibial artery can be seen in (e), and the resulting improved blood flow to the foot in (f).

Fig. 5 represents an observed distinct microcirculation change of

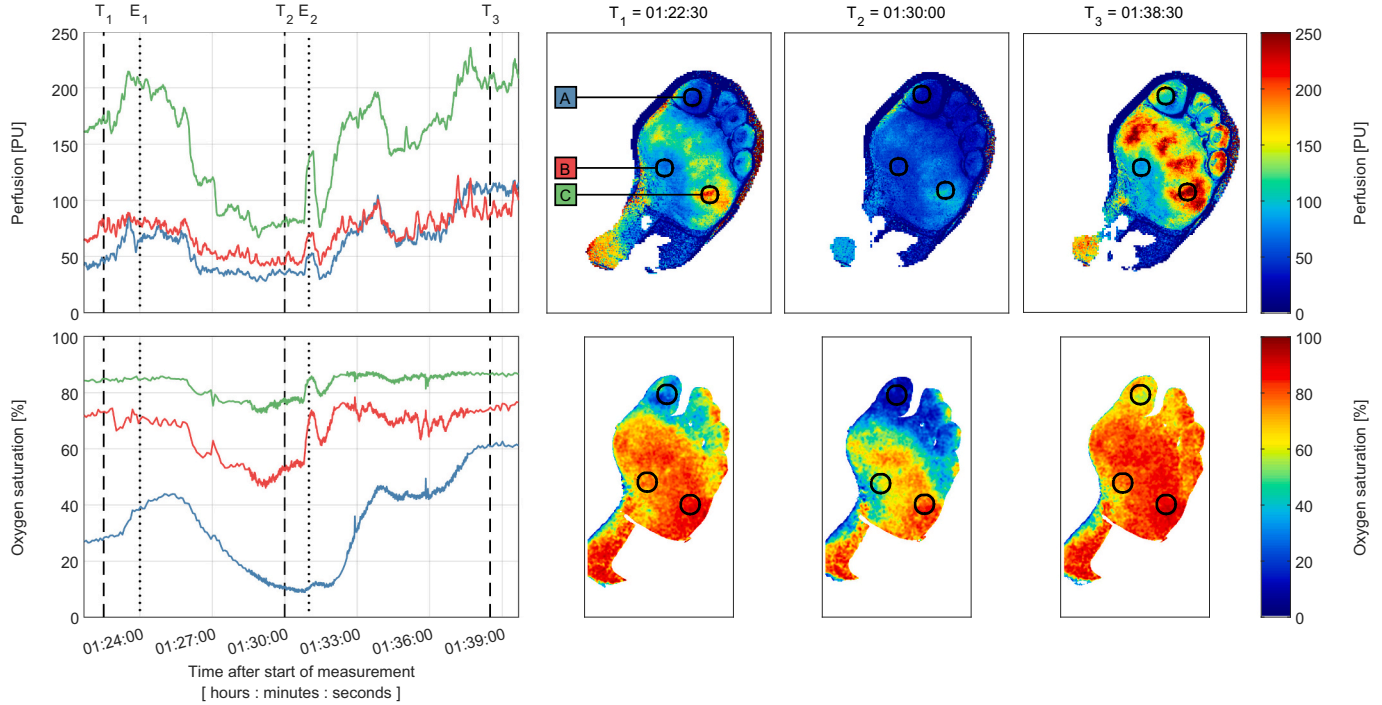

Fig. 3. Case 1. Application of DEB in the anterior tibial artery, resulting in a decrease and subsequent increase of perfusion and oxygen saturation in the foot. The catheter was inserted in the vessel at E_1, and the balloon deflated at E_2. Time-points T_1-T_3 are shown in the perfusion and oxygen saturation images. The oxygen saturation in the 1st toe shows a persistent improvement by approximately 30 percentage units compared to before the DEB.

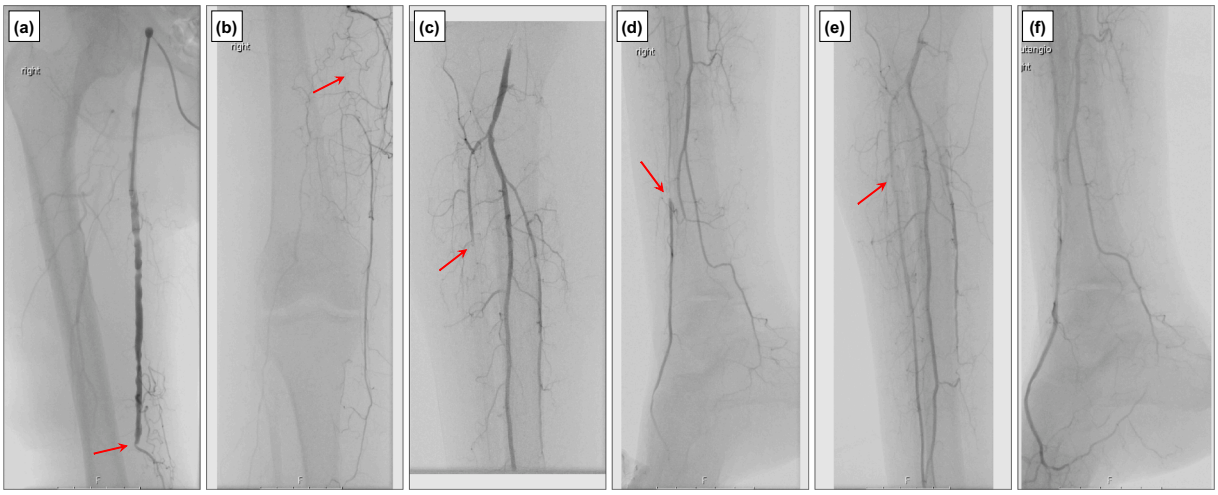

Fig. 4. Case 2. Digital subtraction angiography showing (a) an occlusion of the superficial femoral artery and (b) popliteal artery. (c) Lower leg and (d) foot before intervention, with occlusion of the anterior tibial artery (c), distally filling from collaterals from the fibular artery (d). Post-intervention angiography shows recanalization of the anterior tibial artery (e) and improved blood flow to the foot (f).

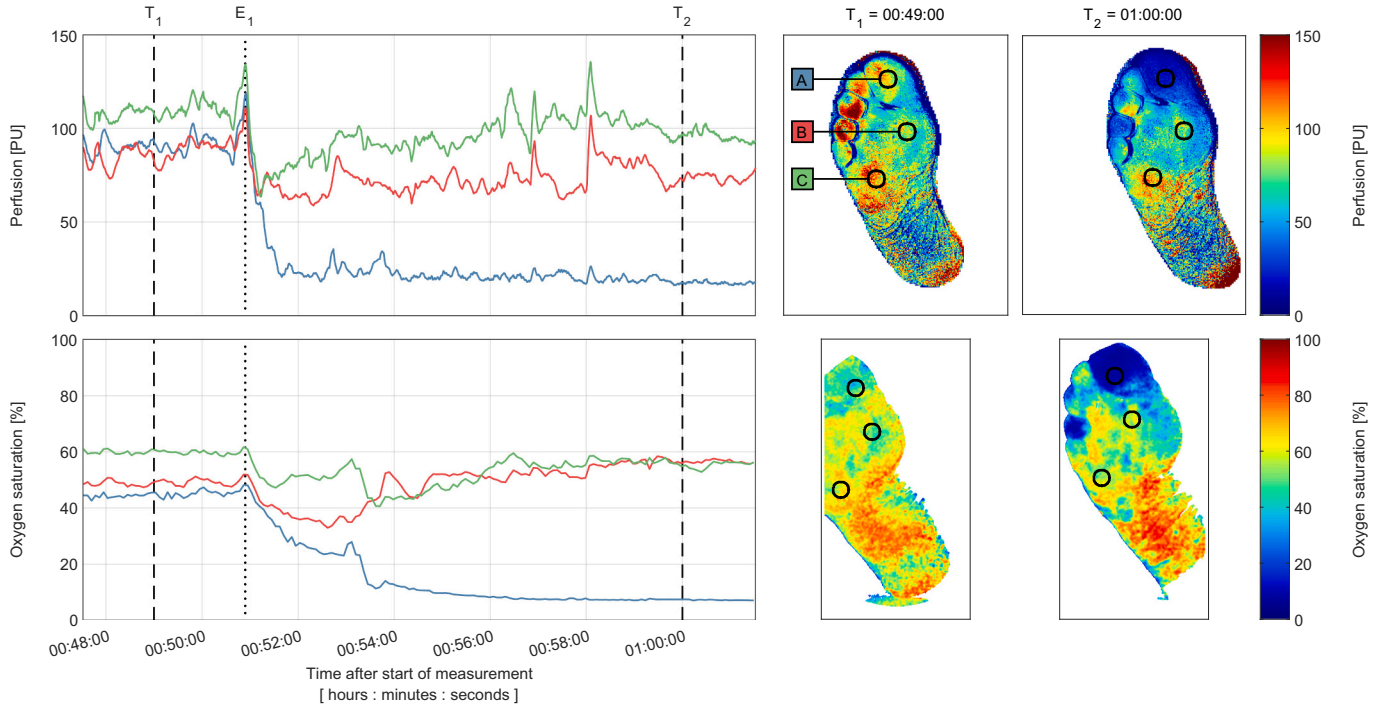

Fig. 5. Case 2. A significant decrease in both perfusion and oxygen saturation following recanalization of the occlusion in the superficial femoral artery and angiography at E_1, indicating localized occlusion in 1st and 4th toe persisting for more than 1 h after the initial onset (outside time-scale of the figure). The patient reported great pain in the 1st toe. A micro-embolization due to the recanalization was suspected.

unknown origin. The change occurs directly after a perioperative angiography at time E_1, following recanalization of the occlusion in the superficial femoral artery and popliteal artery. A sharp decrease in perfusion and a gradual decrease in oxygen saturation is observed, locally in the 1st and 4th toe. Approximately 20 min after this, the patient reports great pain in the 1st toe. A distal embolization was suspected.

Fig. 6 shows the increase in perfusion and oxygen saturation following the release of a balloon dilation in the anterior tibial artery at time E_1 followed by intra-arterial administration of 0.25 μg nitroglycerin at time E_2. Two distinct reperfusion responses are visible in both perfusion and oxygen saturation curves following the two events, with a particularly strong response in the perfusion curves after nitroglycerin administration. The patient reports at time E_3 that the foot is feeling better than before.

Fig. 7 compares the levels and pulsatility of the perfusion and oxygen saturation before and after the intervention (on the operating table), as well as during a routine revisit 13 weeks later. ROIs were selected as in Figs. 5 and 6, with matching ROI colors. Data for these results were not median filtered, to preserve the pulsatile signal. Note that although the perfusion levels in the red and green ROIs are slightly lower during the revisit compared with preintervention levels, the pulsatile nature of the perfusion is clearly visible at the revisit, while absent or indistinguishable from noise before the intervention. The high perfusion level for the

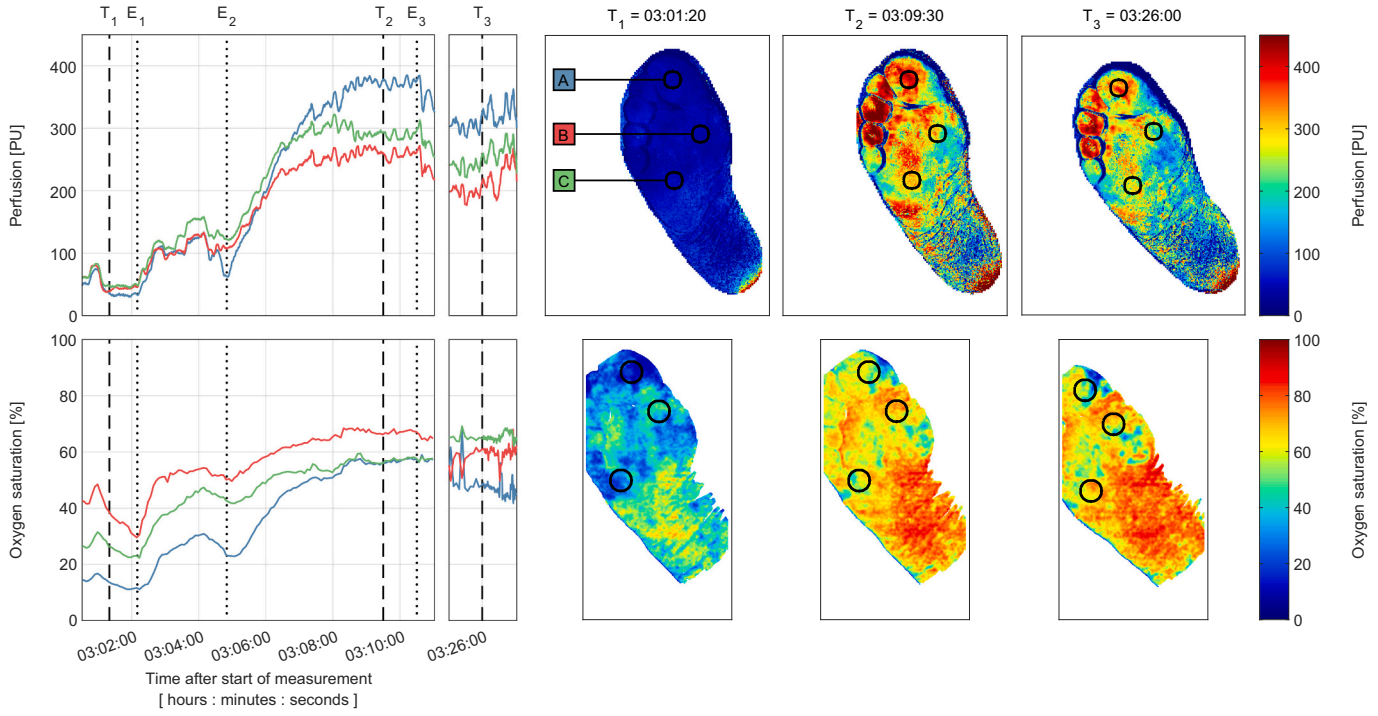

Fig. 6. Case 2. Two subsequent reperfusion responses following the release of a balloon dilation in the arterial tibial artery at E_1 and intravenous nitroglycerin administration at E_2. The patient reports that the foot is feeling better than before at E_3. Note that the color scale in the perfusion images differs from the color scale in Fig. 5.

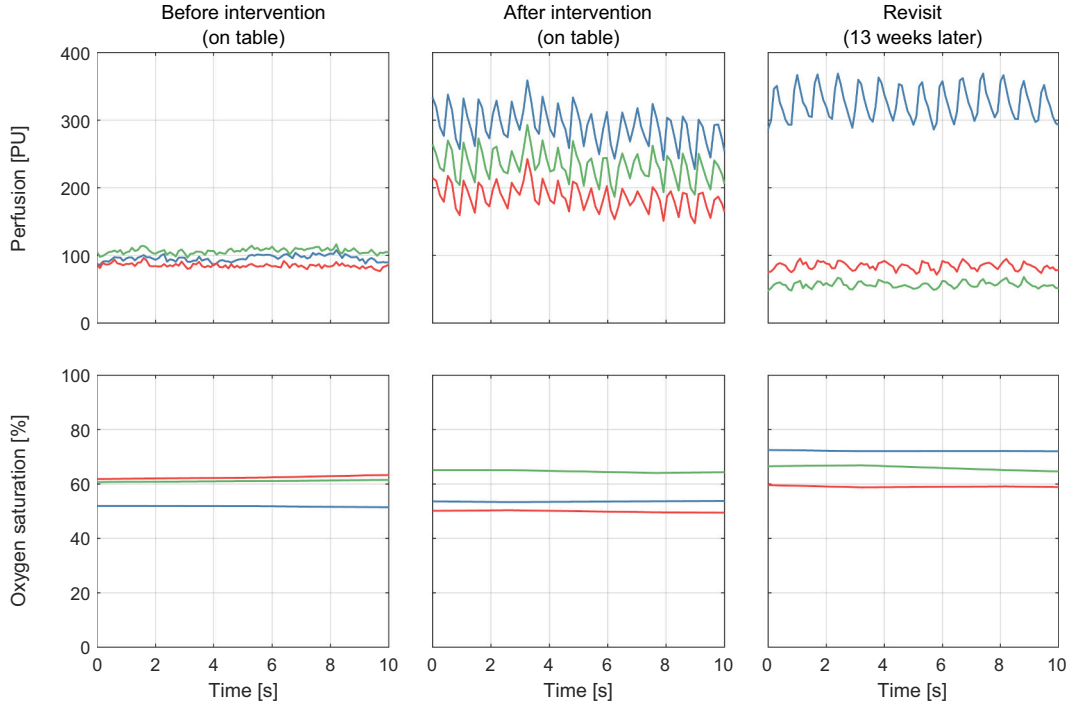

Fig. 7. Case 2. Perfusion and oxygen saturation in 10-second windows directly before and after the intervention, as well as during a revisit 13 weeks later. ROIs are located on the 1st toe (blue), forefoot below 1st toe (red), and forefoot below digit 4–5 (green), matching the ROI placement in Figs. 5 and 6. Note that the high perfusion in the blue ROI during the revisit is due to local heating during preceding measurements of TBI. The red and green ROIs were not affected by this and reflect the normal tissue state.

1st toe (blue ROI) at the revisit is due to local heating during a preceding measurement of the toe-brachial index (TBI). The other ROIs were not affected by this. The patient reported no rest pain at the revisit and her right ankle ABI showed an increase from non-measurable (ABI = 0, no detectable flow signals with Doppler ultrasound), to an ABI = 0.87.

3.3. Case 3

The patient was a 77-year-old man with a clinical history of ischemic heart disease and diabetes. He reported rest-pain (Rutherford 4) for both legs. Preoperative duplex ultrasound showed multiple stenoses in SFA and popliteal artery. Stenoses from middle of SFA to popliteal artery were treated with 6 mm POBA. A stenosis in popliteal artery (segment p3) was then treated with a 5.5 mm woven self-expanding stent. A 4 mm drug-eluting stent (DES) was placed in the popliteal artery (segment p3). Stenoses at multiple levels in the anterior tibial artery was treated with 2.5 mm POBA, and a 3 mm balloon-expandable stent was placed in the origin and midst of the anterior tibial artery, followed by the application of two 2.5 mm DES. Proximal parts of peroneal artery were treated with 2.5 mm POBA.

Fig. 8 shows a distinct change in the microcirculation of unknown cause. A sharp decrease in both perfusion and oxygen saturation followed the intra-arterial administration of carbon dioxide (CO_2) during a perioperative angiography at time E_1. The dramatic reduction in perfusion and oxygen saturation can still be seen in most of the foot more than 90 min later at time T_3. Note however that there are sporadic locations in the foot with high perfusion and oxygen saturation, as well as a few spots with high oxygen saturation but low perfusion. While the triggering event is clear from the data, the physiological explanation of the observed heterogeneity is unknown.

3.4. Case 4

The patient was a 71-year-old man with a clinical history of hypertension and diabetes, and reported rest-pain (Rutherford 4) in the left foot. Preoperative ABI was 0.29 on the left foot, while toe pressure was unmeasurable on the left foot and 31 mmHg on the contralateral foot. Preoperative duplex ultrasound showed multiple stenoses in SFA and an in-stent stenosis in a stent placed in distal SFA during a previous intervention. A post-stenotic duplex signal and suspected stenoses were observed in the popliteal artery. Angiography confirmed these findings and SFA was treated (proximal to distal) with woven self-expanding stents (6 mm and 5.5 mm) and a 4 mm DEB in the previous stent, followed by 5 mm DEBs in distal SFA and popliteal artery. Angiography showed a dissection in the bifurcation of the fibular and posterior tibial artery which was treated with a 3 mm balloon-expandable stent.

Fig. 9 shows spatially distinct patterns of unknown origin in both the perfusion images and oxygen saturation images. The changes occur at time E_1 and remain 1 h later (T_3), although only slightly visible in the perfusion images. As in Case 3, the physiological explanation of the heterogeneity is unknown.

Fig. 10 shows the pulsatility in three ROIs directly before and after the intervention, as well as during a revisit after six months. The data in these ROIs were not median filtered, to preserve the pulsatile signal. An increased pulsatility in the perfusion at the revisit compared to before the intervention is noticeable, as well as high oxygen saturation at both instances. This is supported by the complementary data from the revisit, where the ABI was 0.58 for both legs and toe pressure 30 mmHg for both legs. Additionally, the patient reported no rest pain or ulcers. The low perfusion and lower oxygen saturation directly after the intervention can be explained by the spatially distinct patterns seen in Fig. 9, which were still present when the intervention was finished.

4. Discussion

Improved techniques for evaluating limb-foot microcirculation can have important clinical implications in the assessment of wound healing properties in conservatively managed wounds and as an on-table decision tool during intervention. The goal is to provide additional information for guidance during the intervention, as well as in the pre- and

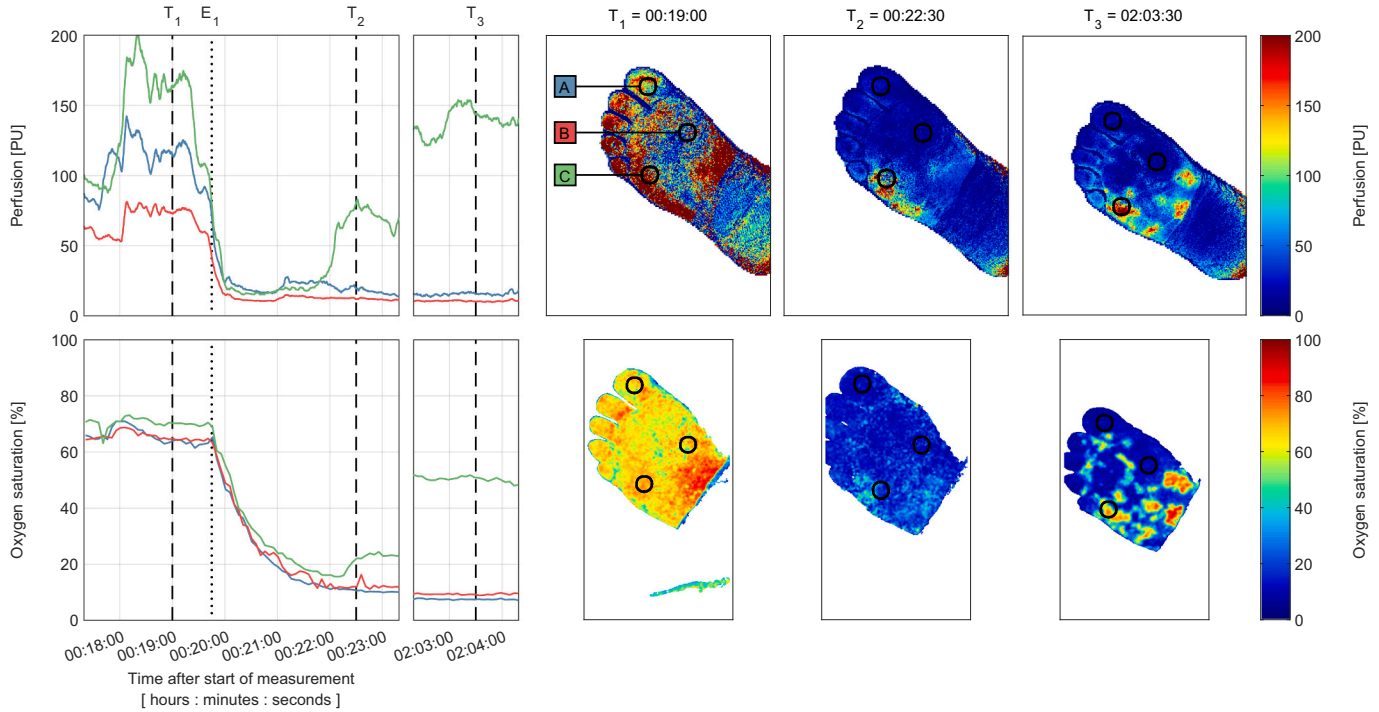

Fig. 8. Case 3. A significant decrease in both perfusion and oxygen saturation following a CO_2 angiography at E_1. The low values persist for more than 90 min (T_3). Sporadic patterns of unknown cause can be observed in the images. Note that the patient has a bandage on the back part of the foot that was not removed by the background masking in the perfusion images.

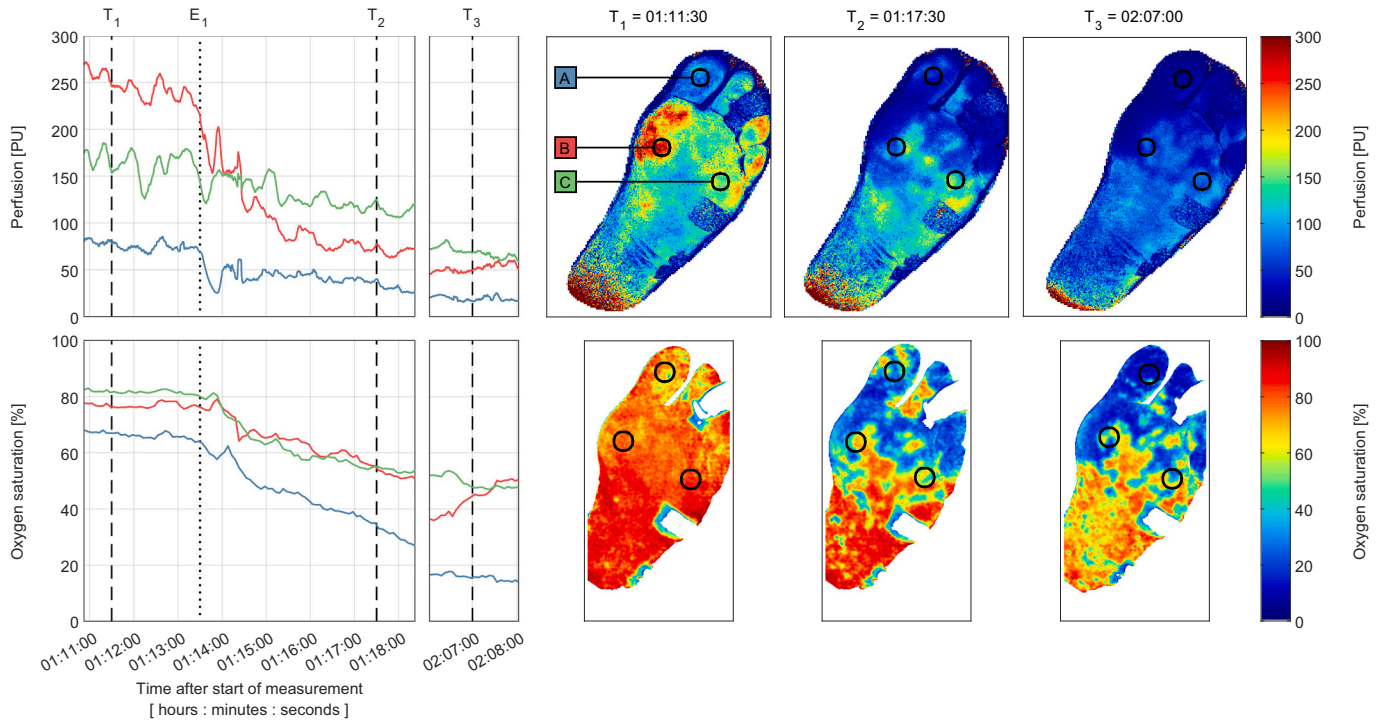

Fig. 9. Case 4. Spatially distinct patterns especially visible in the oxygen saturation images, beginning at E_1 and persisting for more than 1 h (T_3) after the initial change. The perfusion displays a similar pattern, but significantly fainter than the oxygen saturation at T_3. The cause of the changes is unknown.

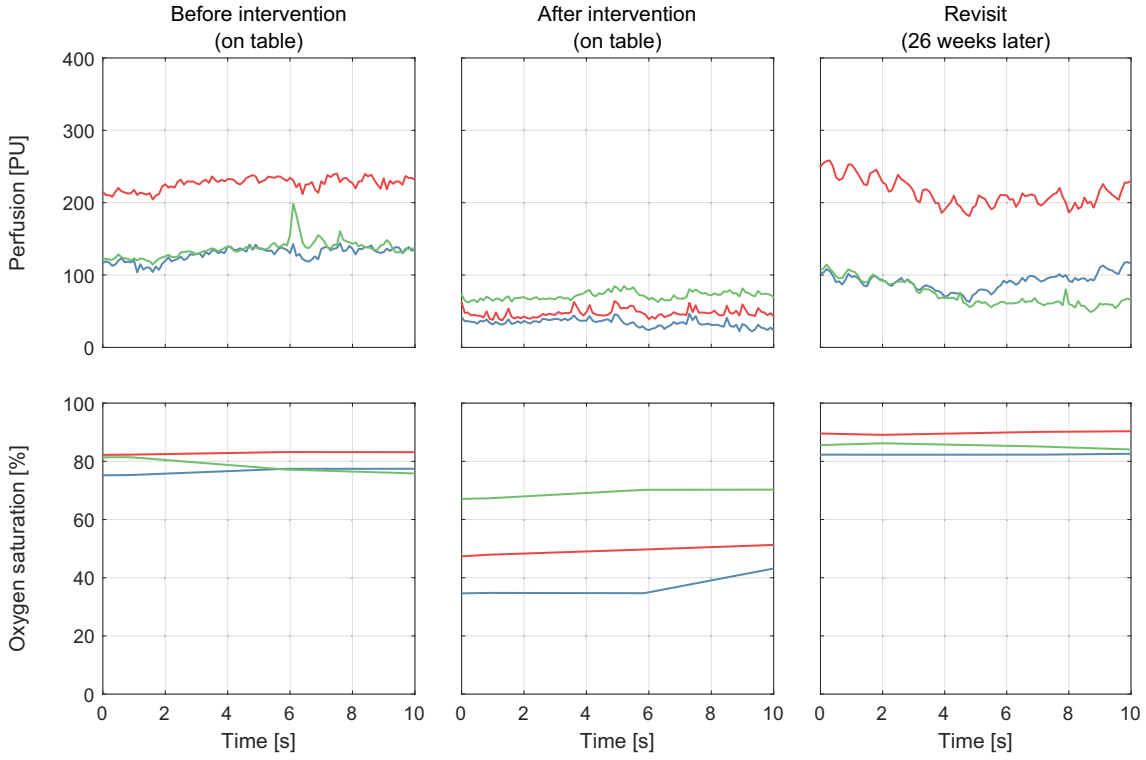

Fig. 10. Case 4. Perfusion and oxygen saturation in 10-second windows directly before and after the intervention, as well as during a revisit six months later. ROIs are located on the big toe (blue), forefoot below big toe (red), and forefoot below digit 4–5 (green), matching the ROI placement in Fig. 9. Note that the spatially distinct patterns seen in Fig. 9 was still present at the end of the intervention, resulting in the abnormally low values of perfusion seen here in the upper middle plot.

post-intervention decision making. In a recent systematic review of peri-operative assessment of tissue perfusion, ten measurement techniques were analyzed for current evidence of their clinical accuracy (Wermelink et al., 2021). The authors concluded that none of the included techniques provided sufficient evidence for clinical adoption and advocated for multi-modal real-time assessment of tissue perfusion and oxygen saturation. The present study shows a novel bio-optical technique for precisely this purpose, demonstrating the *technical* feasibility of peri-operative imaging of microcirculatory perfusion and oxygen saturation, during intervention for CLTI. While pre- and post-operative studies have been done previously, this is the first peri-operative study of this nature. As such, we do not demonstrate the *clinical* feasibility of the technique in this study. This requires a significantly larger sample size and a more strict protocol than the present study.

The selected parts of the interventions presented in this study demonstrate a wide range of spatiotemporal dynamics in the measured microcirculation and were selected as being representative of the overall data. Figs. 3 and 6 were selected based on known events in the interventions, mimicking the potential future use as a tool to display real-time microcirculation improvements or lack thereof following POBA and the placement of stents, to make informed decisions based on both the macro- and microcirculation. For example, in Fig. 3 we observe an increase of 30 percentage units in the oxygen saturation in the 1st toe following the balloon dilation, which persist for the remainder of the intervention. Occlusion-induced reactive hyperemia in the normal population typically persists for shorter times (Jonasson et al., 2020), suggesting this might be due to a persistent improvement in the feeding artery. Similarly, we observe two subsequent increases in perfusion and oxygen saturation following balloon dilation and administration of nitroglycerin as a vasodilator, respectively, in Fig. 6. These are the expected responses to the respective provocations, and further demonstrate that the system can detect relevant dynamics in the microcirculation.

Fig. 5 shows what appears to be a complete occlusion of the 1st and 4th toe following the recanalization of the occlusion in SFA, very similar to the response to arterial occlusion provocations in the healthy population (Jonasson et al., 2020). Worth noting is that the toe-occlusion does not appear immediately following the recanalization, but a few minutes later directly following an angiography using an intravenous contrast agent. One possible explanation is dislodgement of microemboli from the lesion treated after flow-restitution. Ochoa Chaar et al. (2017) analyzed more than 10,000 percutaneous angioplasty procedures for the prevalence and effect of distal embolization. They found an incidence of 3.2% in patients with CLTI. Boc et al. (2020) performed a similar analysis and found an incidence of approximately 1–2%, depending on the patient group. They also found that among the patients with distal embolization, a majority required additional interventions. The embolization suspected in the current patient was probably smaller than those reported in the mentioned studies as it dissolved spontaneously and did not require an additional intervention. Although the event may be infrequent, intraoperative detection is of great importance to allow for immediate additional treatment when necessary.

Figs. 8 and 9, like Fig. 5, demonstrate changes in the microcirculation that were not expected from the preceding intervention. Both figures show significant decreases in perfusion and oxygen saturation with localized skin areas with high values of both quantities. In Fig. 8, the change is rapid and directly follows a CO_2 angiography. The initial decrease is likely an effect of the blood being displaced by the CO_2 used as contrast agent, but this alone does not explain the persistence of the low values for more than 90 min. It is worth noting that the patient experienced increased pain during this time, further supporting the low values seen in the data. Reports of pain have been observed in other studies using CO_2 angiography (Conte et al., 2019). In Fig. 9 the change is slower, and there is no obvious connection to any event during the intervention. The microcirculatory patterns are strikingly similar, especially in the oxygen saturation images.

In addition to the long-term changes in perfusion and oxygen saturation, we present short-term pulsatility graphs in Fig. 7, from directly before and after the Case 2 intervention, as well as at a later follow-up visit to the clinic. While there was no significant change in oxygen saturation levels in this case, we observed a distinct improvement in the perfusion waveforms directly following the intervention. This is probably a reperfusion effect from removing the catheter, but we also observe the improved pulsatility at the revisit. Here we can see the heat-induced hyperperfusion, similar to the perfusion observed directly after the intervention, but also the improved pulsatility in the unprovoked parts of the foot. We present the same pulsatility comparison for Case 4 in Fig. 10. Like the previous case, we observe a distinct improvement in pulsatility in the perfusion signal from before the intervention compared to the revisit. We also observe that there is no significant change in the oxygen saturation. Unlike Case 2, however, the post-intervention graphs show abnormally low perfusion and oxygen saturation values. We attribute this to the spatially heterogeneous pattern seen in Fig. 9, which was still present at the end of the intervention. Regardless of the cause, this clearly demonstrates the value of the spatial information to detect this abnormality since, as we can see in Fig. 9, a slight change in the ROI position might cause large changes in the recorded values. Without the spatial information, false conclusions about the microcirculatory status easily arise.

The algorithms for computing the perfusion images and oxygen saturation images have been presented in previous studies (Hultman et al., 2020; Ewerlöf et al., 2021; Fredriksson et al., 2020). However, the perioperative setting introduced several challenges that had to be addressed for this study to be possible. Especially, foot motion was a major challenge. Quick micro-movements cause perfusion spikes, a known limitation of laser speckle-based techniques. This can be partially alleviated, as in this study, by median filtering the data. One measurement was excluded due to excessive motion artifacts, where median filtering was not sufficient. While motion artifacts are problematic, the almost constant motion seen in this data is rare. In future research, automatic detection of motion artifacts should be investigated, to enable analysis of undisturbed data. It would also be possible to ask the patient to be still at relevant time-points. This would allow snapshot comparisons even in cases such as the excluded one.

Slow movements of the foot also introduce challenges since the positions of ROIs change over time, making automatic analysis difficult. In a lab setting, or in pre- and post-operative measurements, the foot can be fixated to address both these problems. However, in the perioperative setting patients often experience pain in the foot, which would likely be worsened by fixating it for several hours. Additionally, the intervention procedure sometimes requires the patient to move the foot, for example during angiography measurements. Instead, we developed a ROI-tracking algorithm based on a deep learning segmentation model and traditional image registration techniques. Both have been presented in a previous work (Öberg and Hulterström, 2021), but this is the first use of the method in a real measurement setting. We can see from the perfusion images that the method is robust, accurately tracking translations (Fig. 5), small rotations (Fig. 6), and small changes in scale (Fig. 8) of the foot. Although the method was applied in post-processing in the current study, special care was taken to allow all parts of the processing to run in real-time, to prepare for future studies. The MSI data allowed for a simpler background removal algorithm based on the spectrum of each individual pixel. As we can see, this method also performs well in all measurements.

The technical requirements of the perfusion and oxygen saturation imaging system should be addressed. Allowing for continuous measurements during the entire intervention is crucial. As we have demonstrated in this study, unexpected events (see Figs. 5, 8, and 9) can occur and persist for a long time. Detecting these changes early and, for example, administer a vasodilator as a countermeasure, could be beneficial for the comfort of the patient and for the continuation of the intervention. In addition to the continuous nature of the measurements,

it is also valuable to have fast sampling of the images, especially the perfusion, since this enables analysis of the blood pulsatility, a clear indicator of improved vessel patency (Kikuchi et al., 2019). As we demonstrate in Fig. 7, the instrument can detect the improved pulsatility following the intervention. The combination of fast and continuous measurements has not been possible with previous MELSCI-systems. It has been possible with LSCI-systems, but as mentioned in the introduction, LSCI-based perfusion has a poorly understood non-linear response to true perfusion and is more influenced by measurement noise (Hultman et al., 2020).

Analysis strategies for choosing time points to observe during the intervention need to be developed. This study clearly shows the importance of event-based monitoring, where time points are given from the intervention procedures, but also that measurement-based monitoring should be performed. However, the latter can be very time consuming and should be aided by automatic tracking of ROIs during the intervention, and alarms or notifications to the interventionist based on thresholds. The details of this should be investigated in future studies.

5. Conclusion

In this study we presented a novel multimodal system for simultaneous imaging of microcirculatory perfusion and oxygen saturation during CLTI interventions. We demonstrated how spatiotemporal changes in these images can be explained by known physiological events during the intervention. To the best of our knowledge, this is the first report of perfusion imaging and oxygen saturation imaging in a perioperative setting for patients with CLTI. The potential of using a comprehensive assessment of the microcirculation in real-time should serve as the basis for future clinical studies.

CRediT authorship contribution statement

Martin Hultman: Methodology, Software, Validation, Formal analysis, Investigation, Resources, Data curation, Writing – Original draft, Writing – Review & editing, Visualization
Sofie Aronsson: Validation, Investigation, Resources, Data curation, Writing – Original draft, Writing – Review & editing
Ingemar Fredriksson: Conceptualization, Resources, Writing – Review & editing, Project administration, Funding acquisition
Helene Zachrisson: Conceptualization, Writing – Review & editing, Supervision, Funding acquisition
Håkan Pärsson: Writing – Review & editing, Supervision
Marcus Larsson: Conceptualization, Resources, Writing – Review & editing, Funding acquisition
Tomas Strömberg: Conceptualization, Resources, Writing – Original draft, Writing – Review & editing, Supervision, Project administration, Funding acquisition.

Declaration of competing interest

Dr. Fredriksson is part-time employed by Perimed AB, which is developing products related to research described in this publication. None of the other authors have disclosable conflicts of interest.

Acknowledgments

This study was financially supported by the Swedish Research Council (Grant No. 2014-6141) and by Sweden's Innovation Agency VINNOVA via the programs Swelife and MedTech4Health (Grant No. 2017-01435 and 2019-01522). The authors would additionally like to thank Martin Hulterström (MSc) and Andreas Öberg (MSc) for their contribution to this project.

References

Antonopoulos, C.N., et al., 2019. Predictors of wound healing following revascularization for chronic limb-threatening ischemia. Vasc. Endovasc. Surg. 53 (8), 649–657.
Boas, D.A., Dunn, A.K., 2010. Laser speckle contrast imaging in biomedical optics. J. Biomed. Opt. 15 (1).
Boc, A., Blinc, A., Boc, V., 2020. Distal embolization during percutaneous revascularization of the lower extremity arteries. Vasa 49 (5), 389–394.
Briers, D., et al., 2013. Laser speckle contrast imaging: theoretical and practical limitations. J. Biomed. Opt. 18 (6).
Chiang, N., et al., 2017. Evaluation of hyperspectral imaging technology in patients with peripheral vascular disease. J. Vasc. Surg. 66 (4), 1192–1201.
Chin, J.A., Wang, E.C., Kibbe, M.R., 2011. Evaluation of hyperspectral technology for assessing the presence and severity of peripheral artery disease. J. Vasc. Surg. 54 (6), 1679–1688.
Conte, M.S., et al., 2019. Global vascular guidelines on the management of chronic limb-threatening ischemia. Eur. J. Vasc. Endovasc. Surg. 58 (1, Supplement) p. S1–S109. e33.
Duff, S., et al., 2019. The burden of critical limb ischemia: a review of recent literature. Vasc. Health Risk Manag. 15, 187–208.
Ewerlöf, M., et al., 2021. Estimation of skin microcirculatory hemoglobin oxygen saturation and red blood cell tissue fraction using a multispectral snapshot imaging system: a validation study. J. Biomed. Opt. 26 (2), 026002.
Fredriksson, I., et al., 2019. Machine learning in multiexposure laser speckle contrast imaging can replace conventional laser doppler flowmetry. J. Biomed. Opt. 24 (1).
Fredriksson, I., Larsson, M., Strömberg, T., 2020. Machine learning for direct oxygen saturation and hemoglobin concentration assessment using diffuse reflectance spectroscopy. J. Biomed. Opt. 25 (11), 112905.
Gunnarsson, T., et al., 2021. Intraprocedural transcutaneous oxygen pressure and systolic toe pressure measurements during and after endovascular intervention in patients with chronic limb threatening ischaemia. Eur. J. Vasc. Endovasc. Surg. 62 (4), 583–589.
Guolan, L., Baowei, F., 2014. Medical hyperspectral imaging: a review. J. Biomed. Opt. 19 (1), 1–24.
Hardman, R.L., et al., 2014. Overview of classification systems in peripheral artery disease. Semin. Interv. Radiol. 31 (4), 378–388.
Hultman, M., et al., 2017. A 15.6 frames per second 1-megapixel multiple exposure laser speckle contrast imaging setup. J. Biophoton. 11 (2).
Hultman, M., et al., 2020. Real-time video-rate perfusion imaging using multi-exposure laser speckle contrast imaging and machine learning. J. Biomed. Opt. 25 (11), 1–15.
Humeau-Heurtier, A., et al., 2013. Skin perfusion evaluation between laser speckle contrast imaging and laser doppler flowmetry. Opt. Commun. 291, 482–487.
Jayanthy, A.K., 2014. Non invasive blood flow assessment in diabetic foot ulcer using laser speckle contrast imaging technique. In: Proc.SPIE.
Jonasson, H., et al., 2020. Normative data and the influence of age and sex on microcirculatory function in a middle-aged cohort: results from the SCAPIS study. Am. J. Physiol. Heart Circ. Physiol. 318 (4), H908–h915.
Katsui, S., et al., 2017. Novel assessment tool based on laser speckle contrast imaging to diagnose severe ischemia in the lower limb for patients with peripheral arterial disease. Lasers Surg. Med. 49 (7), 645–651.
Katsui, S., et al., 2018. In patients with severe peripheral arterial disease, revascularization-induced improvement in lower extremity ischemia can be detected by laser speckle contrast imaging of the fluctuation in blood perfusion after local heating. Ann. Vasc. Surg. 48, 67–74.
Khaodhiar, L., et al., 2007. The use of medical hyperspectral technology to evaluate microcirculatory changes in diabetic foot ulcers and to predict clinical outcomes. Diabetes Care 30 (4), 903–910.
Kikuchi, S., et al., 2019. Laser speckle flowgraphy can also be used to show dynamic changes in the blood flow of the skin of the foot after surgical revascularization. Vascular 27 (3), 242–251.
Mennes, O.A., et al., 2019. Assessment of microcirculation in the diabetic foot with laser speckle contrast imaging. Physiol. Meas. 40 (6), 065002.
Mennes, O.A., et al., 2021. The association between foot and ulcer microcirculation measured with laser speckle contrast imaging and healing of diabetic foot ulcers. J. Clin. Med. 10 (17), 3844.
Misra, S., et al., 2019. Perfusion assessment in critical limb ischemia: principles for understanding and the development of evidence and evaluation of devices: a scientific statement from the American Heart Association. Circulation 140 (12), e657–e672.
Nouvong, A., et al., 2009. Evaluation of diabetic foot ulcer healing with hyperspectral imaging of oxyhemoglobin and deoxyhemoglobin. Diabetes Care 32 (11), 2056–2061.
Öberg, A., Hulterström, M., 2021. Semantic segmentation using convolutional neural networks to facilitate motion tracking of feet: for real-time analysis of perioperative microcirculation images in patients with critical limb thretening ischemia. In: Department of Biomedical Engineering. Linköping University: DiVA.

Ochoa Chaar, C.I., et al., 2017. Distal embolization during lower extremity endovascular interventions. J. Vasc. Surg. 66 (1), 143–150.
Parthasarathy, A.B., et al., 2008. Robust flow measurement with multi-exposure speckle imaging. Opt. Express 16 (3), 1975–1989.
Shu, J., Santulli, G., 2018. Update on peripheral artery disease: epidemiology and evidence-based facts. Atherosclerosis 275, 379–381.
Thompson, O.B., Andrews, M.K., 2010. Tissue perfusion measurements: multiple-exposure laser speckle analysis generates laser Doppler–like spectra. J. Biomed. Opt. 15 (2), 027015-027015.
Varela, C., et al., 2017. The role of foot collateral vessels on angiosome-oriented revascularization. Ann. Transl. Med. 5 (21), 431-431.
Wermelink, B., et al., 2021. A systematic review and critical appraisal of peri-procedural tissue perfusion techniques and their clinical value in patients with peripheral arterial disease. Eur. J. Vasc. Endovasc. Surg. 62 (6), 896–908.
Zölei-Szénási, D., et al., 2015. Enhancements on multi-exposure LASCA to reveal information of speed distribution. J. Eur. Opt. Soc. 10.